3448 *J. Phys. Chem. A* **2005,** *109,* 3448−3453

Chiroptical Properties of 2-Chloropropionitrile

Kenneth B. Wiberg,*,† Yi-gui Wang,† Shaun M. Wilson,† Patrick H. Vaccaro,† and James R. Cheeseman‡

Department of Chemistry, Yale University, New Haven, Connecticut 06520-8107, and Gaussian, Inc., 340 Quinnipiac Street, Building 40, Wallingford, Connecticut 06492

Received: November 30, 2004

(*S*)-(−)-2-Chloropropionitrile has been prepared from (*S*)-(+)-alanine, and the ORD curves have been obtained in several solvents and in the gas phase. A reaction field extrapolation of the solution data to the gas phase led to an estimated value of $[\alpha]_D = -21°$, whereas the interpolated gas phase value is −8°. The specific rotation was found to be temperature dependent in ethylcyclohexane solution over the range 0−100 °C. Although rotation of the methyl group leads to large calculated effects on the specific rotation, it does not lead to the temperature dependence. Rather, a low frequency mode at 224 cm^{-1} was found to be responsible. This is a mixed mode involving methyl torsion and C−C≡N bending. The specific rotations calculated at the B3LYP/aug-cc-pVDZ level including electric field dependent functions are in very good agreement with the measured gas phase values.

1. Introduction

In an examination of the temperature dependence of the specific rotation for compounds having only one conformation, we found some (α-pinene, camphene) to have a negligible temperature dependence, whereas others gave a positive temperature dependence (camphor) or a negative temperature dependence (*β*-pinene, *cis*-pinane, fenchone).[1] These effects must be due to vibrational modes, and the effects of such modes can be quite large.[2] This group of molecules has large numbers of vibrational modes, making a detailed computational study difficult. Therefore, we are examining other smaller compounds that may give temperature dependent specific rotations and allow a more facile examination of the effect of their vibrational modes. In the first of these studies, we have examined 2-chloropropionitrile, one of the smallest of the chiral molecules.

2. Specific Rotation and Medium Dependence

2-Chloropropionitrile (**1**) has not previously been reported in chiral form. The (*S*)-(−) form was prepared by converting (*S*)-(+)-alanine to (*S*)-(−)-2-chloropropionic acid.[3] The acid (95% ee) was converted to the (*S*)-(−)-amide (**2**) via the acid chloride and reaction with ammonia in ether solution. Recrystallization from ethyl acetate−hexane raised the specific rotation by a small amount, and further recrystallization had no significant effect ($[\alpha]^{25}_D = -21.7$ ($l = 1$, $c = 0.0428$ g/mL, 95% ethanol)). Thus, the amide is believed to have close to 100% ee. Treatment of the amide with phosphorus pentoxide, heating the mixture in an oil bath at ∼210 °C,[4] led to distillation of **1** in good yield, but the product thus obtained was largely racemic. When the dehydration was carried out by heating the flask with a free flame and distilling the nitrile under reduced pressure as it was formed followed by redistillation (bp 116−117 °C), it had $[\alpha]^{25}_D = -13.5$ ($l = 1$, neat, $d = 1.02$ g/mL).

To determine whether some racemization occurred under these conditions, **1** was converted back to the amide with basic hydrogen peroxide in aqueous acetone,[5] which should not lead to racemization. After the reaction was completed, all volatile material was removed under reduced pressure, and the amide was extracted from the solid using chloroform. Evaporation of the chloroform gave **2**. It was ground to a fine powder, and a representative sample was taken and found to have $[\alpha]^{25}_D = -20.1$ ($l = 1$, $c = 0.0432$ g/mL, 95% ethanol). This corresponds to 93% of the maximum rotation, indicating that **1** had 93% ee. The NMR spectrum of another sample found **2** to be 99+% pure. Thus, the maximum rotation of neat (−)-**1** is estimated to be $[\alpha]^{25}_D$ −14.5.

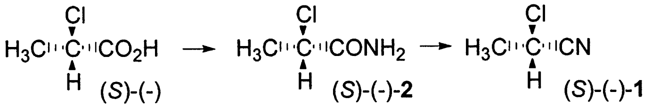

The gas phase specific rotation is a particularly important quantity, since it can be directly compared with the results of theoretical calculations and provides the reference point for solvent effect measurements. It has been determined using the CRDP[6] method, giving $[\alpha] = -6.8 \pm 2.3$ at 633 nm and $[\alpha] = -37.9 \pm 2.9$ at 355 nm (both values corrected to 100% ee). The interpolated value at 589 nm is −8.3.

The ORD curves for **1** in several solvents corrected to 100% ee are shown in Figure 1, and the measured values are recorded in Table 1. It might be noted that some compounds such as methyloxirane show rather large solvent effects on the specific rotation.[7] The rotation of **1** was determined in cyclohexane, di-*n*-butyl ether, acetone, acetonitrile, benzene, and methanol. The solvent effects were relatively small, except for benzene that also gives a rather large solvent effect for methyloxirane.[7]

In other studies of the solvent effect on equilibria[8] or rates of reaction,[9] we have found that cyclohexane, di-*n*-butyl ether, acetone, and acetonitrile usually give solvent effects that are in agreement with a reaction field model and extrapolate to the observed gas phase values, whereas it is known that solvents such as benzene and carbon tetrachloride that have zero dipole moments but large polarizabilities and quadrupole moments usually give a larger than expected solvent effect.

---

† Yale University.
‡ Gaussian, Inc.

10.1021/jp0407371 CCC: $30.25

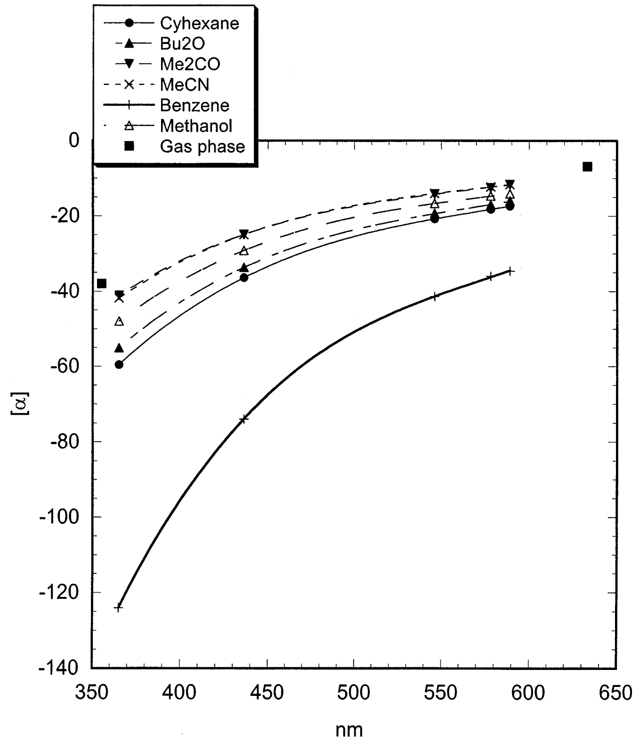

Figure 1. ORD curves for 2-chloropropionitrile in several solvents and in the gas phase. The acetone and acetonitrile curves are almost superimposable. The same is true with cyclohexane and ethylcyclohexane.

TABLE 1: Effect of Solvent on the Specific Rotation of 2-Chloropropionitrile[a]

	nm				
medium	589	578	546	436	365
vapor[b]	−8.3	−8.7	−10.2	−19.8	−34.6
neat	−14.48	−15.16	−17.36	−30.87	−51.35
cyclohexane	−17.35	−18.19	−20.75	−36.34	−59.52
ethylcyclohexane	−17.69	−18.48	−21.13	−37.11	−59.87
di-*n*-butyl ether	−16.01	−17.01	−19.33	−33.63	−55.05
acetone	−11.80	−12.41	−14.14	−24.90	−41.03
acetonitrile	−11.63	−12.24	−13.99	−24.95	−41.74
benzene	−34.58	−39.13	−41.39	−73.93	−124.04
methanol	−14.06	−14.67	−16.65	−28.89	−47.88

[a] The observed values are corrected to 100% ee. The concentration was 0.05 g/mL. [b] Interpolated values, experimental values are for 633 and 355 nm.

A common characteristic of reaction field models is that the calculated results are related to the Onsager dielectric constant function, $(\epsilon - 1)/(2\epsilon + 1)$. Figure 2 shows a plot of the observed specific rotations at 589 nm in cyclohexane, di-*n*-butyl ether, acetone, and acetonitrile as a function of the Onsager parameter. There is a fairly good linear relationship, but extrapolation to zero (gas phase) gives a value that has a considerably larger magnitude than the experimental values. This suggests there may be a fundamental difference between optical rotations determined in the gas phase and those determined in solution. It is interesting that the gas phase specific rotation is closer to the acetonitrile solution value than that found in cyclohexane. Additional examples will be presented in another context.

3. Temperature Dependence of the Specific Rotation

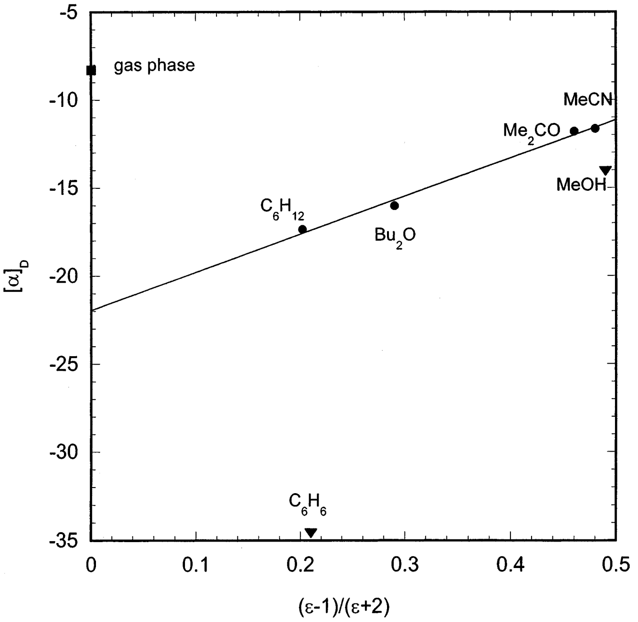

Figure 2. Correlation of the specific rotation with the Onsager function, $(\epsilon - 1)/(2\epsilon + 1)$. At 589 nm extrapolation to the gas phase where the function becomes zero gives −21°, whereas the experimentally derived value is −8°.

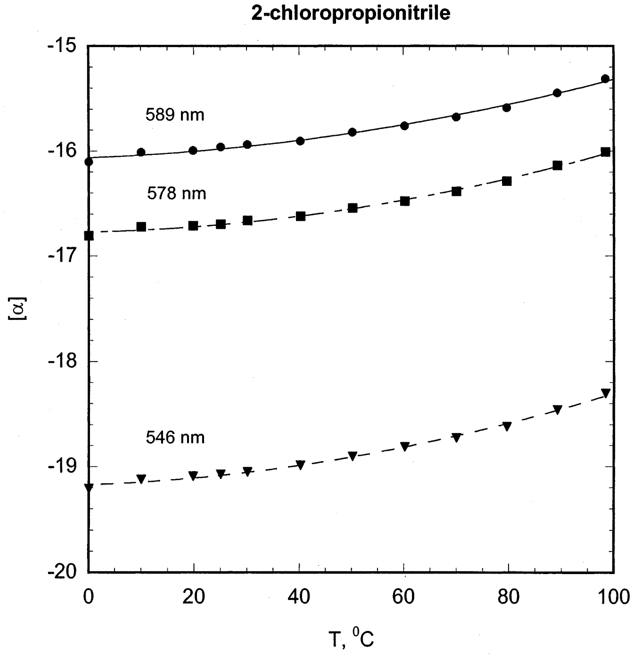

Figure 3. Temperature dependence of the specific rotation at 589, 578, and 546 nm.

One of the major reasons for examining **1** is that it is a relatively simple compound that might exhibit a temperature dependent optical rotation. The rotation was measured in ethylcyclohexane solution from 0 to 100 °C and was corrected for the thermal expansion of the solvent. The experiment was replicated three times, giving consistent results. The data are summarized in Figure 3. There is a temperature dependence, but unlike the other compounds we have studied, the dependence increases somewhat with increasing temperature. Since **1** exists as a single conformer, the most likely source of the temperature dependence is the change in excitation of vibrational modes with increasing temperature.

4. Calculated Specific Rotations

The specific rotation of **1** was calculated with B3LYP and several basis sets using GIAOs to minimize origin effects, giving

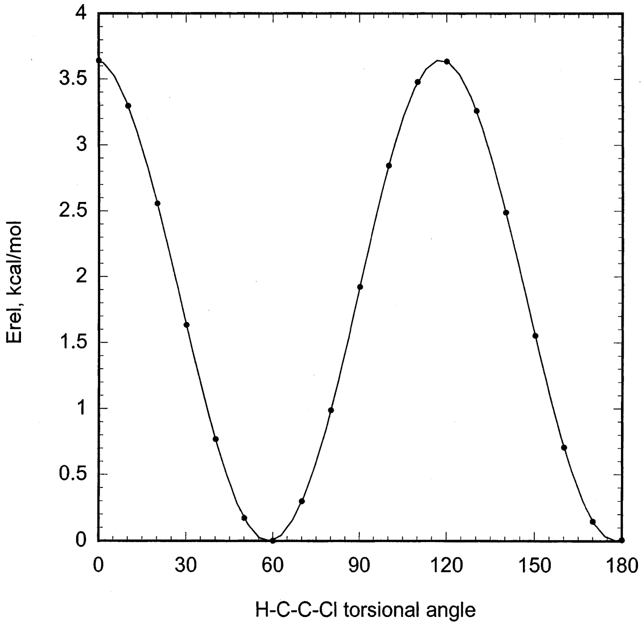

Figure 4. Energy profile for rotation of the methyl group of 2-chloropropionitrile.

TABLE 2: 2-Chloropropionitrile, Optical Activity Calculations

a. No Electric Field Dependent Functions

nm	6-31+G*	6-311++G**	aug-cc-pVDZ	aug-cc-pVTZ
633	−27.68	−17.74	−12.69	−16.09
589	−32.59	−20.92	−15.05	−19.02
578	−34.03	−21.86	−15.75	−19.89
546	−38.84	−24.98	−18.10	−22.78
436	−67.42	−43.71	−32.57	−40.32
365	−109.57	−71.74	−55.33	−67.16
355	−118.92	−78.01	−60.57	−73.26

b. with Electric Field Dependent Functions

nm	6-31+G*	6-311++G**	aug-cc-pVDZ	observed
633	−22.74	−8.23	−8.99	−6.8 ± 2.3
589	−26.38	−10.23	−10.47	
578	−27.43	−10.85	−10.90	
546	−30.89	−12.96	−12.33	
436	−50.04	−27.41	−20.56	
365	−75.70	−52.43	−32.51	
355	−81.17	−58.34	−35.21	−37.9 ± 2.9

the values shown in Table 2. In earlier work,[10] we found that the inclusion of electric field dependent functions[11] led to systematically more satisfactory calculated specific rotations. This was found to be true in the present case. As found with other small molecules, the aug-cc-pVDZ basis set gives more satisfactory calculated specific rotations than does 6-311++G**, and the inclusion of electric field dependent functions significantly improved the calculated specific rotations. The use of aug-cc-pVDZ and these functions leads to a very good agreement with the observed gas phase values.

5. Effect of Methyl Rotation on the Calculated Specific Rotation

The only conformational flexibility in **1** is the rotation of the methyl group. The energy associated with this rotation was calculated at the B3LYP/6-311++G** level, giving the result shown in Figure 4. As expected, there is a 3-fold barrier with minima close to 60 and 180°. The rotational barrier is 3.6 kcal/mol.

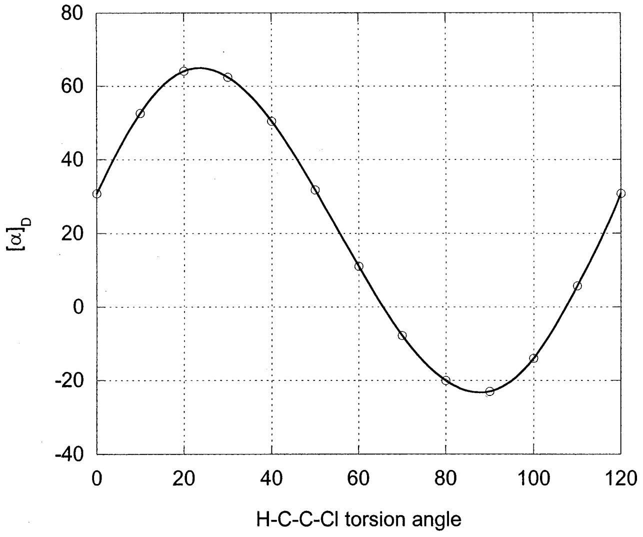

Figure 5. Effect of rotation of the methyl group of 2-chloropropionitrile on the calculated specific rotation.

The effect of methyl rotation on the calculated specific rotation was obtained at the B3LYP/aug-cc-pVDZ level using the structural data obtained in calculating the rotational profile. The rotations calculated for 589 nm are summarized in Figure 5. The curve corresponds to a periodic function, and at ~60°, the minimum in the potential energy, the curve is essentially linear. Since only the curvature contributes to the observed specific rotation, we conclude that methyl rotation has little effect on the optical rotation.

Marked conformational effects on the specific rotation have been observed for other molecules such as 3-chloro-1-butene,[2] hydrogen peroxide,[12] and alanine.[13]

In an effort to obtain more information on the origin of the effect of the H−C−C−Cl torsional angle on the specific rotation, we have examined the tensor components of the rotation. In common with most spectroscopic properties, the observed quantity depends on the orientation of the molecule with respect to the plane of polarization of the incident light. This leads to a ***G′*** tensor, and the calculated rotation is derived from the average of the three diagonal tensor components, G'_{xx}, G'_{yy}, and G'_{zz}. Thus,

$$G'_{\alpha,\beta} = -2\omega \sum_{n\neq 0} \mathrm{Im}\frac{\langle 0|\mu_{\alpha}|n\rangle\langle n|m_{\beta}|0\rangle}{{\omega_{n0}}^{2} - \omega^{2}}$$

where the first term in the numerator is the electric transition moment and the second term is the magnetic transition moment and α and β may be *x*, *y*, or *z*. The sum is taken over all of the excited states. Then, the specific rotation, [α], is given by

$$[\alpha] \propto \beta = -\frac{1}{3\omega}(G'_{xx} + G'_{yy} + G'_{zz})$$

Although the calculated specific rotation is independent of the orientation of the molecule, the individual ***G′*** tensor components are strongly affected by the orientation. Therefore, it is necessary to minimize reorientation of the molecule when the effect of conformation on ***G′*** is examined.

The geometries obtained from the calculation of the torsional potential were used. They were transformed so that the chiral carbon was at the origin, the methyl carbon was on the *z* axis, and one of the groups attached to the chiral center was placed

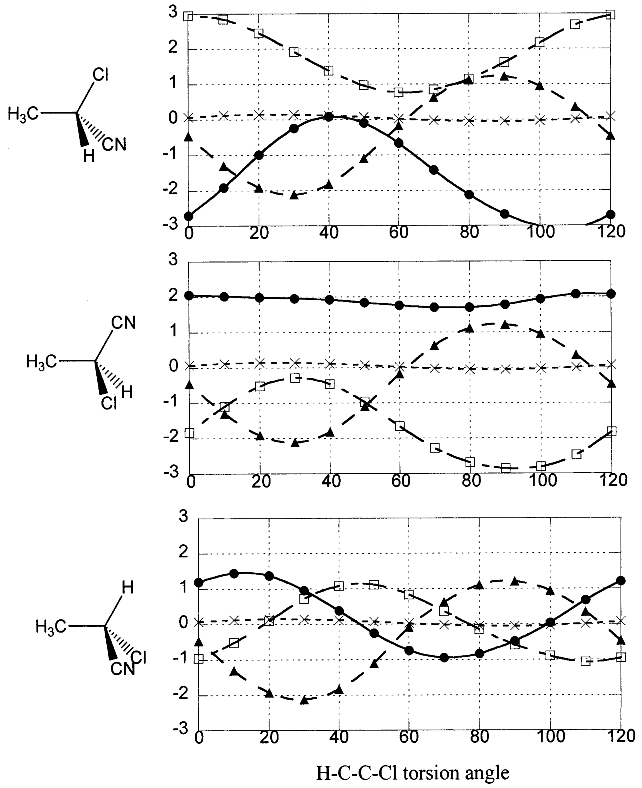

Figure 6. The G' tensor components of the specific rotation for the methyl torsion mode. In each case, the z axis is defined by the C−Me bond and the in-plane substituent lies in the x direction. G'_{xx} is given by the closed circles, G'_{yy}, by the open squares, G'_{zz}, by the triangles, and β, by the crosses. The units of the tensors are atomic units.

in the xz plane. The tensor components derived from these geometries are shown in Figure 6 as a function of the H−C−C−Cl torsional angle. The $\boldsymbol{G}'$ tensor components are clearly periodic functions. The value of β is also shown.

The plots illustrate one of the difficulties in accurate calculations of specific rotations, which are directly related to β. The sum of the tensor components is essentially zero, and thus, β is the small difference between large quantities. A very high accuracy in calculating the $\boldsymbol{G}'$ tensor is needed in order to obtain reasonable accuracy in calculating the specific rotation.

The $\boldsymbol{G}'$ tensor values depend on which of the three groups attached to the chiral center is placed in the xz plane. Although it may not be immediately obvious, they can be interconverted via an appropriate transformation matrix. Only the diagonal terms contribute to the specific rotation, but the off-diagonal terms are mixed in when a coordinate transformation is carried out.

Since the $\boldsymbol{G}'$ tensor components are much larger than the specific rotation, it should be easier to calculate the tensors than the specific rotations on a state-by-state basis. Many of the needed terms can be obtained as part of TDDFT calculations of excited states. However, the magnetic terms need to be calculated using GIAOs so that the results will be gauge independent. In addition, the optical rotation of oriented samples includes a contribution from the electric dipole−quadrupole polarizability tensor which is traceless and thus vanishes for freely rotating molecules.

$$-\omega A_{\alpha\beta\gamma} = -\omega \sum \epsilon_{\alpha\gamma\delta}\omega_n \frac{\langle 0|\mu_\beta|n\rangle\langle n|Q_{\gamma\beta}|0\rangle}{{\omega_n}^2 - \omega^2}$$

where Q is the electronic quadrupole moment operator. This term is purely anisotropic and vanishes upon orientational averaging. We are currently trying to implement such a study so that the excited states that give the major contributions to the tensor and to the specific rotation can be identified.

6. Vibrational Modes for Chloropropionitrile and Their Effect on the Specific Rotation

There is a reported vibrational spectrum of 2-chloropropionitrile,[14] but an examination of the paper shows that the compound studied was 3-chloropropionitrile. The structure and vibrational frequencies for **1** were calculated at the B3LYP/6-311++G** level, which usually gives very satisfactory estimates of the frequencies.[15] The structure is compared with that determined via microwave spectroscopy[16] in Table 3, and the vibrational frequencies are given in Table 4. The MP2 calculated structural parameters are in somewhat better agreement with the experimental structures than B3LYP. The latter does give fairly good calculated values except for a somewhat long C−Cl bond. Since the specific rotation will be calculated using B3LYP, the latter geometries will be used for consistency.

The nature of the vibrational modes was obtained by an examination of an animation of the modes. Since the molecule has little symmetry, many of the modes involve a number of internal coordinates, and the description given is only approximate. The infrared spectrum was examined in carbon tetrachloride and in carbon disulfide solutions. The observed frequencies were assigned on the basis of the positions and relative intensities found in the calculations and are included in Table 4. There is generally good agreement between the calculated and observed frequencies, except for the usually anharmonic C−H stretching modes. For the study in the next section, it was helpful to have information on the anharmonicity of the vibrational modes. An anharmonic frequency calculation[17] was carried out, and the results are included in Table 4. It can be seen that the anharmonic frequencies are in good accord with the observed CH stretching frequencies, and the remainder of the calculated frequencies are also satisfactory. The anharmonicity of the lower frequency modes is relatively small.

We wished to examine the effect of the vibrational mode on the specific rotation. Since the specific rotations were to be calculated at the B3LYP/aug-cc-pVDZ level, the vibrational modes were also calculated at this level. It led to only minor differences in calculated frequencies with respect to B3LYP/6-311++G** (compare Tables 4 and 5). The normal coordinate displacement for a given vibrational mode was calculated from the corresponding mean-square value:[18]

$$\langle Q^2\rangle_n = \frac{h}{4\pi^2 c\omega}\left(n + \frac{1}{2}\right)$$

where the standard deviation (as root-mean-squared displacement), ΔQ_i, is given by

$$\Delta Q_n = (\langle Q^2\rangle_n - {\langle Q\rangle_n}^2)^{1/2}$$

with $\langle Q\rangle_n = 0$ by definition.

The occupancy of higher-lying vibrational levels was taken into account by thermally averaging $\langle Q^2\rangle_n$ over a Boltzman distribution, resulting in a frequency and temperature dependent hyperbolic cotangent function, coth($hc\omega/2kT$).[18] Approximating ω by the calculated vibrational frequency, ν, in reciprocal centimeters and introducing the physical constants, one obtains[19]

$$\Delta Q = \pm((16.8576/\nu) \times \coth(0.719\,384\nu/T))^{1/2}$$

TABLE 3: Calculated and Observed Structural Parameters

parameter	obs	MP2/6-31G**	MP2/6-311++G**	B3LYP/6-311++G**	B3LYP/aug-cc-pVDZ
R(C—Cl)	1.791(10)	1.792	1.790	1.827	1.831
R(C2—C3)	1.523	1.519	1.524	1.527	1.527
R(C2—C1)	1.459	1.465	1.465	1.460	1.465
R(C≡N)	1.159	1.182	1.161	1.153	1.161
∠C1—C2—C3	111.2(10)	111.60	111.65	112.48	112.64
∠C3—C2—Cl	110.9(10)	110.67	110.50	110.74	110.70
∠C1—C2—Cl	109.8(10)	109.65	109.33	108.98	108.76
∠C2—C≡N	180.0	178.42	177.37	177.96	177.98

TABLE 4: Chloropropionitrile Vibrational Modes, B3LYP/6-311++G**

mode	harmonic (cm^{-1})	int (km/M)	k (mdyne/A)	μ (amu)	anharmonic (cm^{-1})	obs (cm^{-1})	description
1	3139	5.6	6.41	1.10	2994	2994	Me CH antisym str, ⊥ to C—C—Cl plane
2	3119	7.3	6.31	1.10	2974	2972	Me CH antisym str, in C—C—Cl plane
3	3096	0.7	6.13	1.09	2953		C—H str
4	3016	6.4	5.66	1.04	2941	2941	Me CH sym str
5	2354	1.1	41.3	12.66	2322	2251	C≡N str
6	1494	3.9	1.37	1.05	1453	1447	Me CH bend
7	1485	9.3	1.35	1.04	1444		Me CH bend
8	1416	5.6	1.43	1.21	1386	1382	Me umbrella bend
9	1336	5.2	1.45	1.38	1302	1307	Me—C—H bend
10	1260	22.2	1.10	1.17	1231	1231	C—C—H bend
11	1115	18.7	1.20	1.65	1089	1086	C—C(N) str and Me wag
12	1091	5.6	1.47	2.10	1061		C—Me str and Me wag
13	1001	17.1	1.09	1.85	986	991	C—Me str and Me wag
14	858	14.5	1.29	2.97	842	852	C—C(N) str and C—Me str
15	674	25.7	1.12	4.20	663	682	C—Cl str
16	557	1.3	0.879	4.80	554	546	Me—C—C(N) bend ⊥ to C—Cl
17	486	8.6	1.68	12.11	481	489	C—Cl str and C—C≡N bend in Cl—C—C(N) plane
18	318	3.0	0.214	3.59	319		Cl—C—Me bend
19	266	0.9	0.059	1.42	257		methyl torsion
20	227	2.6	0.064	2.11	224		methyl torsion and C—C≡N bend ⊥ to C—Cl
21	174	5.7	0.151	8.46	174		C—C≡N bend in Cl—C—C(N) plane

TABLE 5: Effect of Vibrations and Temperature on the Specific Rotation at 589 nm[a]

ν	$[\alpha]_D$ 273+	$[\alpha]_D$ 273−	$[\alpha]_D$ 373+	$[\alpha]_D$ 373−	$\alpha_{ii}^{(2)}$, 273	$\alpha_{ii}^{(2)}$, 373
170	26.97	−1.22	29.33	−3.42	0.59	0.75
224	46.14	−15.99	51.37	−19.79	4.99	6.42
261	23.80	1.21	25.27	−0.36	−0.15	−0.25
318	16.43	9.55	16.91	9.26	0.82	1.01
483	16.00	9.06	16.30	8.75	−0.10	−0.11
550	28.05	−2.56	29.12	−3.58	0.33	0.38
670	23.01	1.71	23.50	1.18	−0.44	−0.48
857	23.84	2.04	24.05	1.77	0.72	0.66
996	18.07	7.17	18.16	7.09	0.08	0.09
1085	13.78	11.34	13.78	11.34	−0.04	−0.04
1105	17.57	7.35	17.57	7.35	−0.24	−0.24
1231	15.01	10.83	15.01	10.83	0.68	0.68
1318	21.03	0.81	21.03	0.81	−3.32	−3.32
1394	11.74	14.01	11.74	14.01	0.59	0.59
1459	18.48	6.21	18.48	6.21	−0.47	−0.47
1468	18.83	7.54	18.83	7.45	1.12	1.12
2345	17.36	8.40	17.36	8.40	0.60	0.60
3051	15.51	9.14	15.51	9.14	−0.51	−0.51
3106	15.90	8.18	15.90	8.18	−1.08	−1.08
3132	33.86	−9.00	33.86	−9.00	−0.30	−0.30
3135	25.33	0.61	25.33	0.61	0.78	0.78
sum					4.65	6.28
no $\nu = 224$					−0.34	−0.14

[a] The specific rotation for the undistorted molecule is 12.58°, and it was calculated at the B3LYP/aug-cc-pVDZ level including electric field dependent functions. The value is slightly different from that given in Table 2 because it used a preliminary value of the electric field dependent term. 273+ and 273− represent positive and negative displacements along the normal coordinate.

and the displacement in Cartesian coordinates is given by

$$\Delta x = \Delta Q/\mu^{1/2}$$

where μ is the reduced mass associated with the vibrational mode. The Cartesian displacements for the given vibrational mode obtained as part of a vibrational frequency calculation (a unit vector) was multiplied by Δx to give the displacement in angstroms. The geometry for the vibrational mode at the positive and negative turning points for the two temperatures was derived from the equilibrium geometry and the rms displacements.

The specific rotations for each of the distorted modes were then calculated (four calculations for each mode, two temperatures and two directions), giving the data summarized in Table 5. The data for one vibrational mode are shown in Figure 7, and it can be seen to be a curve and to have a large range of specific rotations. The magnitude of the temperature effect and the curvature for each of the modes may be seen in Table 5.

A linear change in specific rotation with vibrational distortion gives no net effect on the specific rotation; only the curvature has an effect. The second-order effect for vibrational mode i is given by[2]

$$\alpha_{ii}^{(2)} = \alpha(0 + \Delta x_i) - 2\alpha(0) + \alpha(0 - \Delta x_i)$$

and the net effect of all of the modes on the specific rotation is given by

$$\alpha = \alpha(0) + \frac{1}{2}\sum_{i=1}^{3N-6} a_{ii}^{(2)}(0)$$

The values of $\alpha_{ii}^{(2)}$ are summarized in Table 5. Two of the modes lead to relatively large values, 224 and 1318 cm^{-1}. The latter has too high an energy to allow a difference between 273 and 373 K, but the former will lead to such a difference. It is interesting to note that if the 224 cm^{-1} mode is left out, the net effect of all of the other vibrational modes is negligible. Therefore, it is clear that the 224 cm^{-1} mode is uniquely

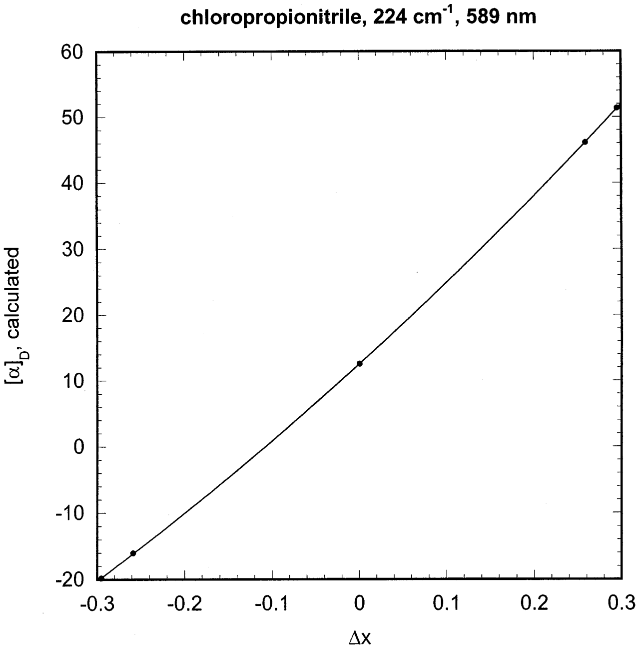

Figure 7. Calculated specific rotation as a function of the displacement, Δx, from the equilibrium geometry for the 224 cm^{-1} vibrational mode. The equation of the curve is $[\alpha]_D = 12.59 + 120.33\Delta x + 36.90\Delta x^2$. $R = 1.000$.

responsible for the observed temperature dependence of the specific rotation.

7. Summary

(1) The calculated specific rotation for **1** is in very good agreement with the observed gas phase values. Most solvents have a small effect on the optical rotatory dispersion, but benzene gives a rather large effect. A reaction field extrapolation of the solution data to the gas phase gives $[\alpha]_D = 21°$, whereas that derived from the gas phase data is $-8°$.

(2) There is an effect of temperature on the specific rotation of **1** in ethylcyclohexane solution. An examination of the effect of the vibrational modes on the specific rotation found that just one mode, at 224 cm^{-1}, is responsible for the temperature dependence.

Calculations. The ab initio calculations were carried out using Gaussian 03.[20] Electric field dependent functions were included for each of the basis sets following the method of Darling and Schlegel.[11] In this method, the center of each Gaussian, A, is chosen to depend on the electric field, ϵ, according to $A(\epsilon) = A - \lambda\epsilon$, where λ is the isotropic field dependent parameter for each shell. The set of λ's for each basis set was chosen to maximize the polarizability of **1**.

Acknowledgment. This investigation was supported by grants from the National Science Foundation.

References and Notes

(1) Wiberg, K. B.; Wang, Y.-g.; Murphy, M. J.; Vaccaro, P. H. *J. Phys. Chem. A* **2004**, *108*, 5559.

(2) Wiberg, K. B.; Vaccaro, P. H.; Cheeseman, J. R. *J. Am. Chem. Soc.* **2003**, *125*, 1888.

(3) Koppenhoefer, B.; Schurig, V. *Organic Syntheses Collective Volume 8*; Freeman, J. P., Ed.; Wiley: New York, 1993; p 119.

(4) Kent. R. E.; McElvain, S. M. *Organic Syntheses Collective Volume 3*; Horning, E. C., Ed.; Wiley: New York, 1955; p 493.

(5) Wiberg, K. B. *J. Am. Chem. Soc.* **1953**, *75*, 3961. Murray, J. V.; Cloke, J. B. *J. Am. Chem. Soc* **1934**, *56*, 2749. McMaster, I.; Noller, C. R. *J. Indian Chem. Soc.* **1935**, *12*, 652.

(6) Müller, T.; Wiberg, K. B.; Vaccaro, P. H. *J. Phys. Chem. A* **2000**, *104*, 5969. Müller, T.; Wiberg, K. B.; Vaccaro, P. H.; Cheeseman, J. R.; Frisch, M. J. *J. Opt. Soc. Am. B* **2002**, *19*, 125.

(7) Kumata, Y.; Furukawa, J.; Fueno, T. *Bull. Chem. Soc. Jpn.* **1970**, *43*, 3920.

(8) Wiberg, K. B.; Keith, T. A.; Frisch, M. J.; Murcko, M. *J. Phys. Chem.* **1995**, *99*, 9072. Foresman, J. B.; Keith, T. A.; Wiberg, K. B.; Snoonian, J.; Frisch, M. J. *J. Phys. Chem.* **1996**, *100*, 16098.

(9) Wiberg, K. B.; Rablen, P. R.; Rush, D. J.; Keith, T. A. *J. Am. Chem. Soc.* **1995**, *117*, 4261. Wiberg, K. B.; Rush, D. J. *J. Am. Chem. Soc.* **2001**, *123*, 2038.

(10) Wiberg, K. B.; Wang, Y.-g.; Vaccaro, P. H.; Cheeseman, J. R.; Trucks, G.; Frisch, M. J. *J. Phys. Chem. A* **2004**, *108*, 32.

(11) Darling, C. L.; Schlegel, H. B. *J. Phys. Chem.* **1994**, *98*, 5855. The $n = 0$ approximation was used.

(12) Polavarapu, P. L.; Chakraborty, D. K.; Ruud, K. *Chem. Phys. Lett.* **2000**, *319*, 595.

(13) Pecul, M.; Ruud, K.; Rizzo, A.; Helgaker, T. *J. Phys. Chem. A* **2004**, *108*, 4269.

(14) Klaeboe, P.; Grundnes, J. *Spectrochim. Acta, Part A* **1968**, *24*, 1905.

(15) Koch, W.; Holthausen, M. C. *A Chemists's Guide to Density Functional Theory*; Wiley-VCH: Weinheim, Germany, 2000.

(16) Ogata, T.; Yamashita, N.; Takata, S. *J. Mol. Struct.* **1997**, *412*, 39.

(17) Barone, V. *J. Chem. Phys.* **2004**, *120*, 3059.

(18) James. R. W. *Z. Phys.* **1932**, *33*, 737.

(19) Cyvin, S. J. *Molecular Vibrations and Mean Square Amplitudes*; Universitets Forlager: Oslo, Norway, 1968; Chapter 5, pp 99−100.

(20) Frisch, M. J.; Trucks, G. W.; Schlegel, H. B.; Scuseria, G. E.; Robb, M. A.; Cheeseman, J. R.; Montgomery, J. A., Jr.; Vreven, T.; Kundin, K. N.; Burant, J. C.; Millam, J. M.; Iyengar, S. S.; Tomasi, J.; Barone, V.; Mennucci, B.; Cossi, M.; Scalmani, G.; Rega, N.; Petersson, G. A.; Nakatsuji, H.; Hada, M.; Ehara, M.; Toyota, K.; Fukuda, R.; Hasegawa, J.; Ishida, M.; Nakajima, T.; Honda, Y.; Kitao, O.; Nakai, H.; Klene, M.; Li, X.; Knox, J. E.; Hratchian, H. P.; Cross, J. B.; Adamo, C.; Jaramillo, J.; Gomperts, R.; Stratmann, R. E.; Yazyev, O.; Austin, A. J.; Cammi, R.; Pomelli, C.; Ochterski, J. W.; Ayala, P. Y.; Morokuma, K.; Voth, G. A.; Salvador, P.; Dannenberg, J. J.; Zakrzewski, V. G.; Dapprich, S.; Daniels, A. D.; Strain, M. C.; Farkas, O.; Malick, D. K.; Rabuck, A. D.; Raghavachari, K.; Foresman, J. B.; Ortis, J. V.; Cui, Q.; Baboul, A. G.; Clifford, S.; Cioslowski, J.; Stefanov, B. B.; Liu, G.; Liashenko, A.; Piskorz, P.; Komaromi, I.;. Martin, R. L.; Fox, D. J.; Keith, T.; Al-Laham, M. A.; Peng, C. Y.; Nanayakkara, A.; Challacombe, M.; Gill, P. M. W.; Johnson, B.; Chen, W.; Wong, M. W.; Gonzalez, C.; Pople, J. A. *Gaussian 03*, revision B.07; Gaussian, Inc.: Pittsburgh, PA, 2003.